New Electric-Field-Driven Mesoscale Phase Transitions in Polarized Suspensions

Anil Kumar,[1] Boris Khusid,[2] Zhiyong Qiu,[1] and Andreas Acrivos[1,*]

[1]*The Levich Institute, The City College of New York, 140th Street & Convent Avenue, New York, New York 10031, USA*

[2]*New Jersey Institute of Technology, University Heights, Newark, New Jersey 07102, USA*

(Received 6 June 2005; published 15 December 2005)

We report the discovery of a new class of an electric field-driven bulk phase transition due solely to dipolar interactions in a suspension under the action of a uniform ac field where the effects of other competing forces are suppressed. This transition appears after the well-known chain-column formation and causes the uniform suspension of columns to rearrange into a cellular pattern consisting of particle-free domains surrounded by particle-rich walls. Interestingly, the characteristic size of these domains scales linearly with the interelectrode spacing and remains insensitive to the size of the particles.

DOI: 10.1103/PhysRevLett.95.258301 PACS numbers: 82.70.Kj, 77.22.Gm, 77.84.Nh

The electric and magnetic manipulation and assembly of polarized particles dispersed in a host fluid find widespread applications, ranging from ferrofluids [1] and electrorheological and magnetorheological suspensions [2–4], to lab-on-a-chip devices [5], and to gels [6]. Although each one of these applications is independently unique, all of them share the common feature of utilizing structural transitions, governed by the dipole-dipole interactions, which decay slowly with the inverse cube of the distance and, depending on the relative orientation of the dipoles, vary from attraction to repulsion. It is well known [7] that, because of such dipolar interactions, polarized particles have a tendency to align rapidly along the field direction and to form chains that subsequently coalesce into thicker columns [8–11]. Inside these columns, the particles then slowly rearrange themselves into body-centered tetragonal structures [12,13]. Although several experimental studies have been performed involving such ''tunable'' anisotropic dipole-dipole interactions, the rich variety of the patterns that have been described could also have been influenced by several additional effects due, for example, to gravity, charge transfer, electrohydrodynamic flow, and thermal convection, which often compete with dipole-dipole forces during the structure formation [13–20]. In contrast, in the present study, all these extraneous effects were minimized, if not eliminated altogether: (a) by using a suspension of neutrally buoyant particles, (b) by employing (ac) fields of high strength, (c) by working with relatively large frequencies where electroconvection is suppressed, and (d) by using a nonconducting fluid to eliminate the effects of any free ions. Thus, an ''ideal'' system was developed for studying the influence of pure dipolar interactions. Surprisingly, a totally new phase transition was observed which, to our knowledge, has never been reported in the past.

The experiments were conducted with a thin layer of a suspension confined between two parallel transparent glass electrodes [Fig. 1(a)] having a large diameter-to-gap ratio. The suspensions were made of neutrally buoyant poly-alpha-olefin spheres (AVEKA, MN) in Mazola corn oil (density 0.92 g/cm^3, viscosity 59.7 cp, and dielectric constant 2.87). The particle and oil densities were matched at 23 °C, thereby eliminating any gravitational segregation of the suspension over the experimental time scales. The suspension concentration was varied from 0.5% (v/v) to 10% (v/v). Two different particle sizes, having diameters 45 and 87 μm, were used, and the interelectrode gap was varied from 0.6 to 3.5 mm. We also varied the shape (circle, square, and hexagon) and the size (cavity diameter, $D =$ 1.5, 2, and 2.5 in.) of the experimental cavity. The electrodes were energized by employing (ac) fields with their root mean square (rms) voltages varying from 1 to 6 kV at frequencies ranging from 0.1 to 3 kHz. This frequency range was chosen so as to suppress electrophoresis, electroconvection, and charge transfer, the strengths of which decrease with increasing field frequency. We also employed two types of glass electrodes (Gray Glass, NY)

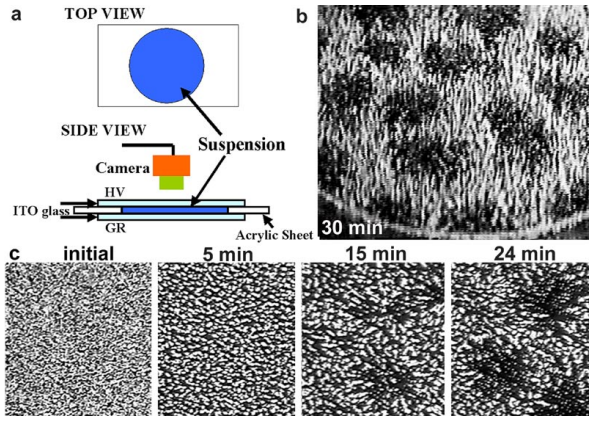

FIG. 1 (color online). Formation of a cellular pattern in the plane perpendicular to the field direction. The particles are seen as white spots and the particle-free domains as black; 87 μm particles, cavity diameter 1.5 in., gap 1.8 mm, 3 kV rms/0.1 kHz. (a) Experimental setup. (b) View from an angle ~30° to the electrodes; 2(v/v)% suspension. (c) Particle rearrangement following the field application; 3(v/v)% suspension.

with different surface properties and found that they did not affect the measurements. The images of the various patterns, which we report below, were quantified using the SIGMASCAN pro 5 (SYSTAT Software, IL). On these images, the particles are seen as white spots and the particle-free domains as black. The fractional area covered by the particles was thus estimated by computing the average gray level (GL) of all pixels of the image, with the GL of a pixel defined as the relative local brightness, having a range from 0 (black) to 255 (white). Hence, the average value $(1 - \mathrm{GL}/255)$ reflects the optical transmittance through the suspension [18].

An important parameter typically used to assess the relative strength of the interparticle forces is $\Lambda = \upsilon_p \varepsilon_0 \varepsilon_f E_{\mathrm{rms}}^2 \Psi_\omega / 4 k_B T$, the ratio of the electric dipolar to thermal energies [21], where υ_p is the particle volume, ε_0 is the vacuum permittivity, ε_f is the liquid dielectric constant, E_{rms} is the rms (ac) field strength, Ψ_ω accounts for the dependence of the relative particle polarization, β, on the field frequency [22], and $k_B T$ is the thermal energy. In our experiments, Λ varied from 6×10^6 to 1.7×10^8, clearly showing that the electrical interparticle forces dominate the thermal forces. For the poly-alpha-olefin particles dispersed in corn oil, we found, using a Novocontrol BDS-80 instrument [23], that $\mathrm{Re}(\beta) = -0.15$ over the frequency range employed, whereas $\mathrm{Im}(\beta)$ decreased rapidly with frequency from 1.8×10^{-3} at 0.1 kHz to less than 2×10^{-4} at 1 kHz. Since the polarizability of the particles did not vary within the chosen frequency range, the insensitivity of our results, to be presented, to the field frequency provides additional evidence that these are due only to interparticle electric interactions.

In a typical experiment (Fig. 1), we found that, for several minutes following the field application, the suspension behavior followed a well-known scenario [2,3,7,12,13] for large Λ. Specifically, almost instantaneously following the application of the (ac) field, the particles aggregated head-to-tail into chains that bridged the gap between the electrodes in the direction of the applied field. These chains, which resemble small aggregates when observed on the plane perpendicular to the direction of the applied field, remained uniformly distributed. In turn, these chains began to coalescence laterally to form thicker multichain columns while still maintaining their uniform spatial distribution [Fig. 1(c)]. After about 10–20 min following the application of the field, we observed a novel, unexpected phenomenon, i.e., the appearance of ''repulsion centers,'' henceforth to be referred to as nuclei, throughout the whole experimental cavity. At these nucleation sites, the particle columns, which had been formed initially, began moving radially outward, without disintegrating, thereby creating particle-free domains spanning the gap between the electrodes. We also found that the process of column coalescence continued as the columns moved radially outward [Fig. 1(c)]. These particle-free domains continued to grow until they interfered with one another, at which point a steady cellular pattern was established. The final columnar structure and the dynamics of such a pattern formation are shown in [Fig. 1(b), supplementary video in Ref. [24]]. We found that, once formed, the suspension patterns remained stable after the electrodes were deenergized, consistent with our assumption that any nonelectrical forces, which would have favored a spatially uniform particle distribution, were of negligible strength. The photo in Fig. 1(b) illustrates the highly inhomogeneous structure of the columns. Also, changes in the shape (circle, square, and hexagon) and the size ($D = 1.5$–2.5 in.) of the experimental cavity had no effect on the structural morphology, i.e., the density of the nucleation sites, except for the regions adjacent to the external boundaries [Fig. 2(a)]. This result, along with the observation that the nucleation sites were randomly distributed inside the experimental cavity, eliminates the possibility that the walls of the cavity were somehow responsible for initiating the nucleation process and therefore establishes the fact that we are dealing here with the existence of a ''bulk nucleation'' phenomenon.

We also measured the average GL value of an image [shown in Fig. 1(c)], taken in the plane perpendicular to the direction of the applied field, in order to estimate the degree of particle alignment along the electric field lines and its evolution. A decrease of GL with time [Fig. 2(b)] indicates that the particles inside the columns realign themselves continuously along the field. Moreover, the observed monotonic variation of GL [Fig. 2(b)], plus the experimental observation that the particle columns moved radially outward without disintegrating, suggests that the particles within the columns continue to realign themselves along the field direction and that the appearance of the nucleation sites and the growth of the particle-free domains involve only the spatial rearrangement of the columns. The GL reached a constant value after about 60 min, this being taken as the final state of our experiments.

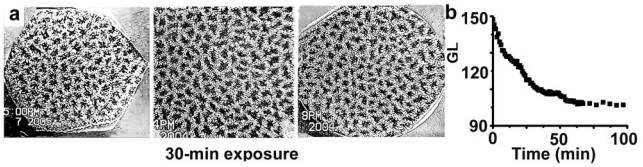

FIG. 2. Characteristics of phase transitions. (a) Cellular patterns formed in hexagonal (side 0.87 in., gap 2.0 mm), square (2 in. $\times$ 2 in., gap 1.8 mm), and circular (diameter 2 in., gap 1.8 mm) cavities. The particles are seen as white spots and the particle-free domains as black; 45 μm particles, 5(v/v)% suspension, 30 min exposure to 3 kV rms/0.1 kHz. (b) Variation of GL with exposure time; 87 μm particles, 1(v/v)% suspension, cavity diameter 1.5 in., gap 3.5 mm, 6 kV rms/0.1 kHz. The nuclei appeared about 16 min following the field application.

Next, we quantified the morphology of the final cellular patterns formed in our experimental cavities. We used images of the patterns in the plane perpendicular to the direction of the applied field [Figs. 1(c) and 2(a)] and employed SIGMASCAN to calculate the main structural features of the pattern, specifically R_c, R_f, and R_{agg}, which refer, respectively, to the mean radius of a cell, the mean radius of the particle-free domain, and the mean radius of a typical column located inside the particle-rich cell walls. The first, $R_c = D/2\sqrt{N}$, was computed by counting, within the experimental cavity of diameter D, the total number of the cells, N, which remained constant since their inception except for a few rare cases when the merging of two neighboring cells was also observed, while R_f was computed from the average area of the particle-free portion of cells [shown by the central black part of the cells in Fig. 2(a)]. Finally, R_{agg} was calculated from the average area of ~100–200 columns randomly chosen within the cell walls [shown by the white spots in Fig. 1(c)]. The schematic representation of these structural parameters is shown in the inset of Fig. 3. We found that, over the full range of our experimental conditions, both R_c and R_f, which were reproducible to within ±(5–7)%, depended strongly on the spacing between the electrodes, L, and on the particle volume fraction of the suspension, c (in v/v), according to $R_c/L = (0.58 \pm 0.04)/c^{0.28\pm0.02}$ and $R_f/L = (0.19 \pm 0.02)/c^{0.48\pm0.02}$, but were insensitive to the particle size, the field strength, and the field frequency. Their insensitivity to the particle size and their linear dependence on L suggests that the transition depicted in Fig. 3 is of the mesoscale type, i.e., at a scale larger than the particle size but comparable to the interelectrode gap. Similarly, R_{agg} and its variance, σ_{agg}, were also unaffected by changes in the particle size, the applied field strength, and the field frequency and were found to depend only on the spacing between the electrodes and the initial concentration of the suspension, according to $R_{agg} = (0.37 \pm 0.06)L^{0.48\pm0.06} \times c^{0.37\pm0.04}$ and $\sigma_{agg} = (0.32 \pm 0.06)L^{0.63\pm0.06}c^{0.40\pm0.05}$, where R_{agg}, σ_{agg}, and L are given in mm. These results for R_{agg} are similar to those in magnetic fluids, where the mean radius of the coalescing columns was also found to be described by a power law $R_{agg} \sim L^{\alpha_L}c^{\alpha_c}$, with $\alpha_L \sim 0.47$ for a 12% ferrofluid [11] and $\alpha_c \sim 0.5$ and $\alpha_L \sim 0.37$ for 4–20(v/v)% magnetic emulsions [8].

Next, to quantify the kinetics of the pattern formation, we measured the time variation of the mean radius of the particle-free domains, R [the black domains in Fig. 4(a)]. We found that, for $t > t_0$, where t_0 denotes the time at which the nuclei first appeared following the application of the electric field, R grew linearly with $(t - t_0)$ initially, but that its rate of increase slowed down when the neighboring nuclei started to interact [Figs. 4(b) and 4(c)]. The fact that the nuclei in our system appeared nearly at once at $t = t_0$, were randomly distributed, and, initially, grew linearly with $(t - t_0)$ motivated us to represent our data according to a phenomenological model, the so-called Kolmogorov-Johnson-Mehl-Avrami (KJMA) model [25], which has been used to describe the kinetics of phase transformations in various systems involving the random nucleation and growth of a new phase. In this model, the evolution of a particle-free domain is given by

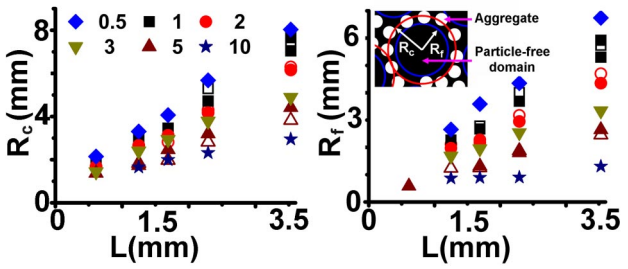

FIG. 3 (color online). Mesoscale nature of the structural transition. The plots show the dependence of the final average radius of the cells, R_c, and the particle-free domains, R_f, as a function of the interelectrode spacing, $L = 0.61$–3.53 mm, and initial particle concentration, $c = 0.5$–10(v/v)%. All the experiments presented in the plots were conducted at the field strength ($E_{rms} \sim 1.7$ kV/mm) and frequency (0.1 kHz) of the applied ac field within a circular cavity of diameter, $D = 2$ in. Various symbols refer to different initial particle concentrations, c (v/v)%. The filled and hollow symbols refer to experiments conducted with 87 and 45 μm-sized particles, respectively. The inset in the right plot shows a sketch of the various structural parameters.

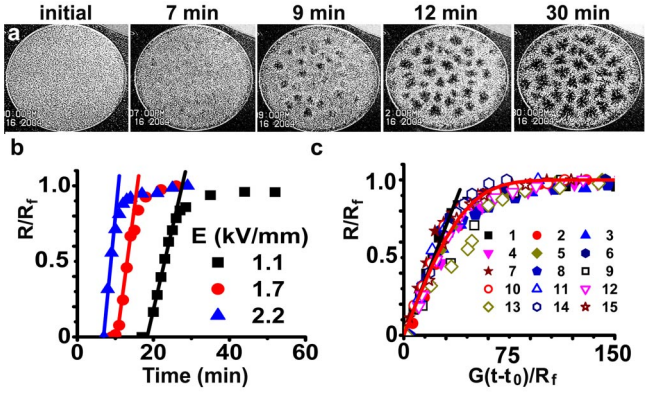

FIG. 4 (color online). Dynamics of the pattern evolution. (a) The particle rearrangement following the application of 3 kV rms/0.1 kHz. The particles are seen as white spots and the particle-free domains as black; 87 μm particles, 2(v/v)% suspension, cavity diameter 1.5 in., gap 1.8 mm. (b) The straight lines show the initial growth of the particle-free domains, R/R_f. (c) Experimental data (symbols) on the growth of the particle-free domains and as predicted by Eq. (1) (solid line). The experimental conditions are listed in the supplementary information [24].

$$R^2/R_f^2 = 1 - \exp[-G^2(t - t_0)^2/R_f^2], \quad \text{so that } R = G(t - t_0) \quad \text{for } R \ll R_f, \tag{1}$$

with G denoting its initial linear growth rate. Our data for the linear part of the R vs $(t - t_0)$ curve shown in Fig. 4(b) yield $t_0 = (5.6 \pm 2.3)/E_{\mathrm{rms}}^{1.4\pm0.2} c^{0.3\pm0.1}$ and $G = (7 \pm 1)E_{\mathrm{rms}}^{1.8\pm0.3}/c^{0.7\pm0.2}$, where t_0 is given in min, G in μm/min, E_{rms} in kV/mm, and c in v/v.

In conclusion, by employing an ideal system in which, aside from dipole-dipole interactions, the effects of all other forces have been suppressed, we have identified a new "bulk" phase transition in suspensions under the action of a uniform ac field. This transition appeared after the well-known chain-column formation and caused the uniform suspension of columns to form a cellular pattern. Interestingly, the structural features of this pattern depended only on the suspension concentration and the interelectrode gap but remained insensitive to the particle size and the field frequency, as well as to the shape and the diameter of the experimental cavity. The growth kinetics of the structure formation was found to be governed only by the applied field strength and the initial particle concentration. We further believe that such phase transitions should be present whenever a system of dipoles is confined between materials of high electric or magnetic susceptibility and the influence of other forces is suppressed. The observed ability to tune the characteristic size of the cellular domains, using the particle concentration and confinement as control parameters, suggests a new means of tuning the interparticle interactions and of manipulating the suspension pattern and offers the potential to develop novel routes for controlling colloids and creating materials with tailored structures. Although the interaction of the dipolar columns has been widely discussed in the literature [8–13], no physical explanation appears to have been provided for the observed spontaneous rearrangement of the columns into a cellular pattern at a scale of L, which thus remains as an open issue in need of further attention. The experimental results that we have presented here should be helpful in providing the necessary framework for understanding such phenomena and developing models for their description.

We are grateful to R. E. Rosensweig, J. L. Lebowitz, G. Drazer, and P. M. Reis for their constructive comments on earlier versions of this manuscript. This work was supported in part by grants from NASA NAG3-2698, NSF CTS-0307099, and NSF/Sandia NIRT/NER-0330703 (B. K). We also express our thanks to A. Zubarev and A. Romanchuk for working with us on computer simulations of the field-driven particle motions supported by NATO Grant No. CLG 976994 (A. A., B. K.).

*Electronic address: acrivos@sci.ccny.cuny.edu

[1] R. E. Rosensweig, *Ferrohydrodynamics* (Cambridge University Press, Cambridge, 1985).
[2] *Progress in Electrorheology. Science and Technology of Electrorheological Materials*, edited by K. O. Havelka and F. E. Filisko (Plenum, New York, 1995).
[3] A. Yethiraj and A. van Blaaderen, Nature (London) **421**, 513 (2003).
[4] J. M. Ginder, APS News **13**, 10 (2004).
[5] M. P. Hughes, *Nanoelectromechanics in Engineering and Biology* (CRC Press, Roca Raton, 2003).
[6] Sh. Yao, U. Beginn, T. Gress, M. Lysetska, and F. Wurthner, J. Am. Chem. Soc. **126**, 8336 (2004).
[7] J. Priestley, *The History and Present State of Electricity with Original Experiments* (J. Dodsley, London, 1769), 2nd ed.
[8] J. Liu, E. M. Lawrence, A. Wu, M. L. Ivey, G. A. Flores, K. Javier, J. Bibette, and J. Richard, Phys. Rev. Lett. **74**, 2828 (1995).
[9] J. E. Martin, K. M. Hill, and C. P. Tigges, Phys. Rev. E **59**, 5676 (1999).
[10] E. M. Furst and A. P. Gast, Phys. Rev. E **62**, 6916 (2000).
[11] H. Wang, Y. Zhu, C. Boyd, W. Luo, A. Cebers, and R. E. Rosensweig, Phys. Rev. Lett. **72**, 1929 (1994).
[12] R. Tao and J. M. Sun, Phys. Rev. Lett. **67**, 398 (1991).
[13] U. Dassanayake, S. Fraden, and A. van Blaaderen, J. Chem. Phys. **112**, 3851 (2000).
[14] M. Seul and D. Andelman, Science **267**, 476 (1995).
[15] R. E. Rosensweig, Magnetohydrodynamics **35**, 305 (1999).
[16] F. Elias, C. Flament, J.-C. Bacri, O. Cardoso, and F. Graner, Phys. Rev. E **56**, 3310 (1997).
[17] K. L. Babcock, R. Seshadri, and R. M. Westervelt, Phys. Rev. A **41**, 1952 (1990).
[18] N. Markarian, M. Yeksel, B. Khusid, A. Kumar, and P. Tin, Phys. Fluids **16**, 1826 (2004).
[19] M. V. Sapozhnikov, Y. U. Tolmachev, I. S. Aranson, and W.-K. Kwok, Phys. Rev. Lett. **90**, 114301 (2003).
[20] M. Trau, S. Sankaran, D. A. Saville, and I. A. Aksey, Langmuir **11**, 4665 (1995).
[21] P. G. de Gennes and P. A. Pincus, Phys. Kondens. Mater. **11**, 189 (1970).
[22] B. Khusid and A. Acrivos, Phys. Rev. E **52**, 1669 (1995).
[23] A. Kumar, Z. Qiu, A. Acrivos, B. Khusid, and D. Jacqmin, Phys. Rev. E **69**, 021402 (2004).
[24] See EPAPS Document No. E-PRLTAO-95-043550 for movies showing dynamics of pattern formation and list experimental conditions for Fig. 4. This document can be reached via a direct link in the online article's HTML reference section or via the EPAPS homepage (http://www.aip.org/pubservs/epaps.html).
[25] P. Papon, J. Leblond, P. Herman, E. Meijer, and S. L. Schnur, *The Physics of Phase Transitions* (Springer-Verlag, Berlin, 2002), p. 423.